



## Identification, synthesis and quantification of process-related impurities in auraptene

Yan-Gang Li, Hai-Fang Chen, Ming-Zhu Tu, Pu-Zhao Zhang, Xiao-Yun Wang, Jin-Bin Yuan, Wu-Liang Yang\*

The Key Laboratory of Modern Preparation of TCM of Ministry of Education, Jiangxi College of Traditional Chinese Medicine, Nanchang, Jiangxi Province, China, 330004

### ARTICLE INFO

#### Article history:

Received 13 October 2010  
Received in revised form 9 May 2011  
Accepted 12 May 2011  
Available online 19 May 2011

#### Keywords:

Auraptene  
Impurity  
Identification  
Synthesis  
Quantification

### ABSTRACT

Impurities in chemically synthesized auraptene, an active pharmaceutical ingredient (API), were detected by a gradient Reverse-Phase High-Performance Liquid Chromatography (RP-HPLC) method. Molecular weights and major product ions of these chemical compounds were determined by Liquid Chromatography/Triple Quadrupole (LC-MS/MS) analysis. Structural assignments were presumed as umbelliferone (Imp-I), (E)-6,7-dihydroxy-3,7-dimethyl-2-octene-umbelliferone (Imp-II), (E)-6,7-epoxy-3,7-dimethyl-2-octene-umbelliferone (Imp-III) and 4-methylauraptene (Imp-IV). The impurities were authentically synthesized, confirmed by Nuclear Magnetic Resonance spectroscopy (NMR) and Infrared spectroscopy (IR), and subsequently used as reference samples in routing HPLC system suitability testing for method specificity and detectability. Method specificity was further verified by forced degradation studies. The developed method was validated for characterization of impurities in synthesized auraptene according to the guidelines of the International Conference on Harmonization (ICH) in our laboratory.

© 2011 Elsevier B.V. All rights reserved.

### 1. Introduction

In recent years, as a citrus coumarin derivative, auraptene was reported to exert *in vivo* and *in vitro* valuable pharmacological properties including anticarcinogenic, anti-inflammatory, antihelicobacter, antigenotoxic and neuroprotective effects [1,2]. Meanwhile, its chemopreventive mechanism was also investigated popularly, e.g. induction of carcinogen detoxifying enzymes, induction of apoptosis, inhibition of free radical generation metalloproteinase, inflammatory pathways and polyamine synthesis [3]. Recently, citrus auraptene has been recognized as an effective chemopreventive agent in rodent models against cancers of liver, skin, tongue, esophagus, colon [4,5], and especially against degenerative diseases. Although pharmacological effect of this chemical is still uncertain in mammals, auraptene may be proposed as a promising drug against a wide range of human diseases in the future.

Synthesis of auraptene has been previously reported in our laboratory [6]. In succeeding preclinical phase trials, pharmacokinetic, pharmaceutical and pharmacological characterization of the synthesized auraptene, as an active pharmaceutical ingredient (API), were completed in our laboratory (data not published). For API produced by organic chemical synthesis, it was believed necessary to isolate and characterize impurities according to

the ICH [7], and various analytical approaches have been used in this respect, e.g. capillary electrophoresis, electron paramagnetic resonance, gas–liquid chromatography, gravimetric analysis, HPLC, solid-phase extraction methods, liquid–liquid extraction method, Ultraviolet Spectrometry, IR spectroscopy, supercritical fluid extraction column chromatography, mass spectrometry, NMR spectroscopy, and RAMAN spectroscopy [8]. Since impurities have been undoubtedly brought into the final pharmaceuticals in auraptene synthetic process, it was believed necessary to fully characterize the impurity profile in various batches of drug substance at release to ensure consistent quality and safety, especially when no reports were available yet on identification, characterization and quantitative determination of process-related substances in chemically synthetic auraptene.

Residual solvents in auraptene have been determined by gas chromatography in our laboratory [9]; they will not be further discussed in this paper. In this paper, impurities formed during the auraptene synthesis process were detected, identified, synthesized, quantified and characterized by various spectroscopic techniques. Validation of the developed analytic procedures was also carried out in accordance with the ICH guidelines.

### 2. Experimental

#### 2.1. Materials and reagents

Samples of auraptene API (no. 20090331, 20090401, 20090409, 20090413 and 20090416) were maintained in our laboratory.

\* Corresponding author. Tel.: +86 791 7118659; fax: +86 791 7118658.  
E-mail address: [yangwuliang@163.com](mailto:yangwuliang@163.com) (W.-L. Yang).

Acetonitrile and methanol (HPLC Grade) were purchased from Merck Chemicals (Shanghai) Co., Ltd. Except for acetonitrile and methanol; all other chemicals including 7-hydroxy-4-methylcoumarin were analytical grade and purchased from Xiya Chemical (Nanjing) CO., Ltd.  $\text{CDCl}_3$  was purchased from Sigma–Aldrich (Shanghai) Trading Co., Ltd.

Reverse osmosis Milli-Q water was used in reagents prepared for mobile phase. All solvents and sample solutions were filtered through 0.22  $\mu\text{m}$  PVDF membrane filters, which were purchased from Tianjin Tengda Filter Equipment Plant of China.

## 2.2. RP-HPLC analysis

Samples of auraptene API were analyzed using a Waters 2695 HPLC system equipped with a 2996 photodiode array detector, and the detection wavelength was set at 324 nm since in our preliminary test that all detectable major products and auraptene had showed maximum absorption wavelength around 324 nm. An Empower PDA software version 2.0 was utilized for system control, data collection and analysis. The flow rate was set at 0.5 mL/min. The mobile phase for pump A was water, for pump B was acetonitrile. A gradient system was employed in the following manner:  $t$  (min)/A (v/v)/B (v/v) = 0/50/50, 5/45/55, 8/24/76, 20/10/90, 30/10/90. Chromatographic separation was achieved on a Diamonsil  $\text{C}_{18}$  column (150  $\times$  4.6 mm i.d., 5  $\mu\text{m}$  particles) using aqueous acetonitrile solution as the mobile phase. The column temperature was maintained at 25 °C. Samples were prepared at 100 mg/mL concentration in methanol. The injection volume for each sample was 10  $\mu\text{L}$ .

## 2.3. LC–MS/MS analysis

LC–MS analysis was performed to identify impurity structures using an Agilent 6410 Triple Quadrupole MS system coupled with an Agilent 1200 Series RRLC system. The RRLC system consisted of an Agilent 1200 Series binary pump SL with degasser, an Agilent 1200 Series autosampler SL, and an Agilent 1200 Series thermostatted column compartment SL. All system components were controlled under the Agilent MassHunter Workstation Software (version: B.01.02). The same chromatographic method described in Section 2.2 was here applied, with the addition of 0.1% formic acid in the water mobile phase A to achieve MS ionization. Samples were run in positive ion electrospray mode, 30 psig nebulizer pressure, and 6 L/min gas flow rate. The source voltage was maintained at 4.5 kV, the drying gas temperature was at 350 °C. A time segment program for the diverter valve was set as: 0–4 min, waste; 4–19 min, MS; 19–22 min, waste; 22–25 min, MS.

## 2.4. Synthesis of auraptene impurity standards

### 2.4.1. Imp-III

A solution of 5 g meta-chloroperoxybenzoic acid (mCPBA) in 80 mL anhydrous dichloromethane (DCM) was added dropwise into a cooled (0 °C) solution of 7.5 g auraptene in 80 mL DCM within 15 min. After stirring at room temperature for 12 h, this solution was washed successively with saturated aqueous  $\text{NaHCO}_3$  and  $\text{H}_2\text{O}$ , and then dried with  $\text{MgSO}_4$ . A colorless oil-like liquid was obtained after solvent evaporation, and purified by 100–200 mesh silica gel column chromatography using 1:1 petroleum ether (bp, 60–90 °C):ethyl acetate as the eluent.

### 2.4.2. Imp-II

1 g of Imp-III was added to a solution of 200 mg concentrated sulfuric acid in 20 mL THF. This mixture was stirred at room temperature for 24 h, poured onto crushed ice. An aqueous layer was collected after THF evaporation, and extracted with DCM. The

DCM layer was washed with aqueous  $\text{NaHCO}_3$  solution, dried with  $\text{MgSO}_4$  and concentrated under vacuum, until a light yellow oil-like product was collected. Then this liquid was purified by 100–200 mesh silica gel column chromatography. A solution of 2:1 petroleum ether (bp, 60–90 °C):ethyl acetate (three times volume of solution than silica gel volume) and a mixture of 1:2 petroleum ether (bp, 60–90 °C):ethyl acetate were successively loaded onto the column as eluents.

### 2.4.3. Imp-IV

Synthesis of Imp-IV was completed in two steps with geranyl bromide as an intermediate. In the first step, 10 g geraniol was thoroughly dissolved in 100 mL anhydrous petroleum ether (bp, 60–90 °C) at 40 °C. Then 5.2 mL Pyridine was put in this solution at –20 °C, mixed with 50 mL solution of 7 g  $\text{PBr}_3$  in anhydrous petroleum ether (bp, 60–90 °C) dropwise over 15 min. This mixture was stirred at –20 °C for 3 h, added with a liquid containing 20 mL water and 40 mL methanol, and stirred once again for 5 min. Subsequently, an organic layer was separated, neutralized with aqueous  $\text{NaHCO}_3$  solution until the pH value reached to 7–8, washed with water, and dehydrated in  $\text{MgSO}_4$ . At last, it was concentrated under vacuum conditions until 8 mL and a colorless oil-like geranyl bromide was collected. In the second step, 8 mL geranyl bromide was added to a solution, which contained 6 g Imp-V, 10.5 g KI and 35.3 g  $\text{K}_2\text{CO}_3$  in 200 mL anhydrous acetone. This mixture was refluxed at 70 °C for 7 h, cooled and filtered at room temperature. After solvent evaporation the product was purified by 100–200 mesh silica gel column chromatography using 2:1 petroleum ether:ethyl acetate as the eluent.

## 2.5. NMR spectroscopy

The NMR spectra of synthesized compounds were collected in  $\text{CDCl}_3$  using a JNM-ECA-400 instrument operating at 400 MHz for  $^1\text{H}$  and 100 MHz for  $^{13}\text{C}$ , respectively. All spectra were acquired at room temperature.  $^1\text{H}$ -NMR spectra were acquired with a 16 kHz sweep width using 64 time domain points with an acquisition time of 4 s.  $^{13}\text{C}$ -NMR spectra were acquired with sweep width variable from 0 to 250 kHz.  $^1\text{H}$  and  $^{13}\text{C}$  chemical shifts were referenced to the residual solvent line at 7.28 ppm and 77.0 ppm, respectively.

## 2.6. IR spectroscopy

The IR spectra for isolated impurities were recorded in the solid state as KBr powder dispersion using a Bruker (VERTEX70) FT-IR spectrometer. Number of sample scan and background scan were set at 32. Resolution was 4.000  $\text{cm}^{-1}$  and spectral window range was 4000–400  $\text{cm}^{-1}$ .

## 2.7. Standard solution preparation

Different amount of the four standards were mixed and dissolved in methanol, stored and protected from light at 4 °C when not in use. The final concentrations in this stock solution were 41.44  $\mu\text{g}/\text{mL}$  for Imp-I, 41.60  $\mu\text{g}/\text{mL}$  for Imp-I, 39.60  $\mu\text{g}/\text{mL}$  for Imp-II and 43.12  $\mu\text{g}/\text{mL}$  for Imp-III. Six different aliquots (0.5, 1.0, 2.0, 3.0, 4.0, 5.0 mL) of this stock solution were transferred into 10 mL volumetric flasks separately, diluted to 10 mL with methanol, and then stirred. Each sample was filtered through 0.22  $\mu\text{m}$  PVDF membranes for LC analysis. The diluted standards of 10  $\mu\text{L}$  were injected into the HPLC.

## 2.8. Preparation of the auraptene samples

Accurately weighed 1 g samples of auraptene API were dissolved completely in warm methanol by sonication. After cooling, each

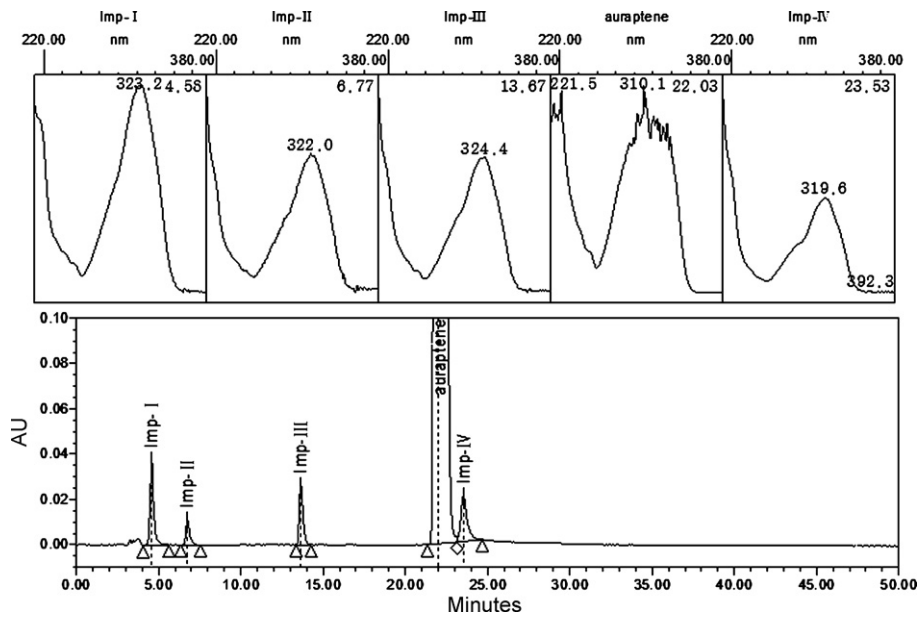


Fig. 1. Chromatogram and UV spectrogram of samples of auraptene API (batch number 20090409).

solution was transferred into 10 mL volumetric flasks, diluted with methanol to the mark, homogenized and then left to settle. Each sample was filtered with the same method described in Section 2.7. The injection volume for each filtered solution was 10  $\mu$ L. The content of each analyte was calculated from the corresponding calibration curve.

### 2.9. Solution preparation for validation of HPLC method

A 10  $\mu$ g/mL stock solution of impurity mixture was prepared by dissolving 1 mg impurities (Imp-I, Imp-II, Imp-III and Imp-IV, respectively) and 1 mg auraptene in methanol in a volumetric flask. Then this liquid was diluted to 1  $\mu$ g/mL as analytical test mixture. This standard solution was used for checking system suitability parameters. A stock solution made up of 200  $\mu$ g/mL auraptene was

used for determining specificity of the HPLC method. To check system precision, the four impurities were mixed together to yield the standard solution, in which the concentration for Imp-I, Imp-II, Imp-III and Imp-IV were 12.432  $\mu$ g/mL, 12.48  $\mu$ g/mL, 11.88  $\mu$ g/mL, and 12.936  $\mu$ g/mL, respectively.

Each sample was filtered with the same method described in Section 2.7, and stored protected from light at 4  $^{\circ}$ C when not in use.

## 3. Results and discussion

### 3.1. Detection of impurities by RP-HPLC

Four impurities in auraptene were detected by a gradient RP-HPLC method. The four target impurities were marked as Imp-I, Imp-II, Imp-III and Imp-IV in the chromatogram and UV spectro-

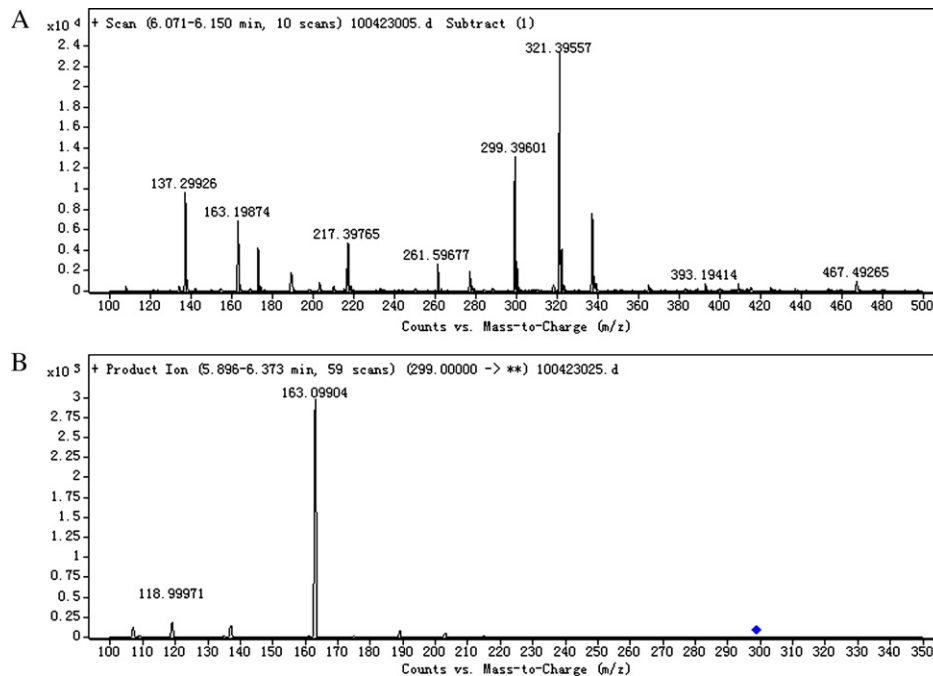


Fig. 2. (A) Mass spectrum and (B) MS/MS spectrum of auraptene.

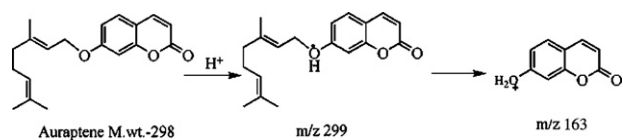


Fig. 3. Fragmentation mechanism for ions  $m/z$  163 formation from auraptene.

gram. Rt for auraptene, Imp-I, Imp-II, Imp-III and Imp-IV were 22.03 min, 4.58 min, 6.77 min, 13.67 min and 23.53 min, and wave length of maximum absorption were 324.4 nm, 323.2 nm, 322.0 nm, 324.4 nm and 319.6 nm, respectively (Fig. 1).

### 3.2. Identification and structural elucidation of impurities

All chemical entities were analyzed by LC-MS/MS method under positive ES ionization conditions. In positive ion full-scan mode, the mass spectrum obtained for auraptene showed two protonated molecular ions, i.e.  $(M+H)^+$  at  $m/z$  299 and  $(M+Na)^+$  at  $m/z$  321 (Fig. 2A). A major product ion ( $m/z$  163) was obtained

from collided precursor ion ( $m/z$  299) (Fig. 2B). Precursor ion ( $m/z$  321) did not yield any characteristic product ions. Formation of the product ion could be explained by the dissociation mechanism of auraptene (Fig. 3).

In positive ion full-scan mode, a protonated molecular ion peak was identified at  $m/z$  163 in the spectrum of Imp-I (Fig. 4). This ion peak was characteristic of umbeliferone, a trace substance originated from unreacted starting material in auraptene synthesis (Fig. 5A). Identity of this impurity was confirmed by HPLC method.

In positive ion full-scan mode, a protonated molecular ion  $(M+Na)^+$  at  $m/z$  337 was identified in the mass spectrum of Imp-III (Fig. 6A). Molecular weight of Imp-III was 314 amu (atomic mass unit), which was 16 amu more than auraptene. As a positive ion originated from Imp-III ( $m/z$  337) fragmentation,  $m/z$  185 was a major product ion with a molecular weight 22 amu more than auraptene ( $m/z$  163) (Fig. 6B). In this case, the product ion from Imp-III was supposed to be sodium adduct of the analogue product ion. Imp-III was thus deduced bearing an extra oxygen atom than auraptene. Since auraptene can be easily oxidized into

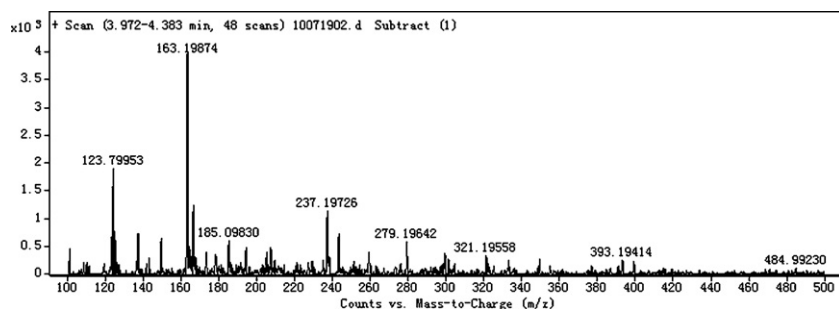


Fig. 4. MS spectrum of Imp-I.

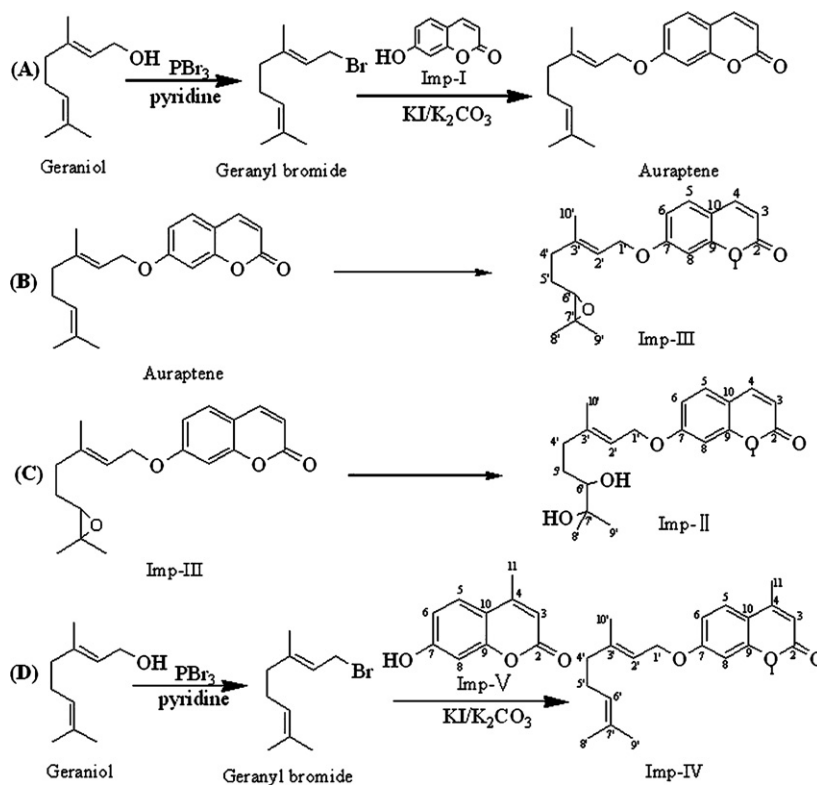


Fig. 5. Scheme for synthesis and NMR assignment of auraptene and impurities. (A) auraptene synthesis and Imp-I formation; (B) formation and NMR assignment of Imp-III; (C) formation and NMR assignment of Imp-II; (D) formation and NMR assignment of Imp-IV and Imp-V.

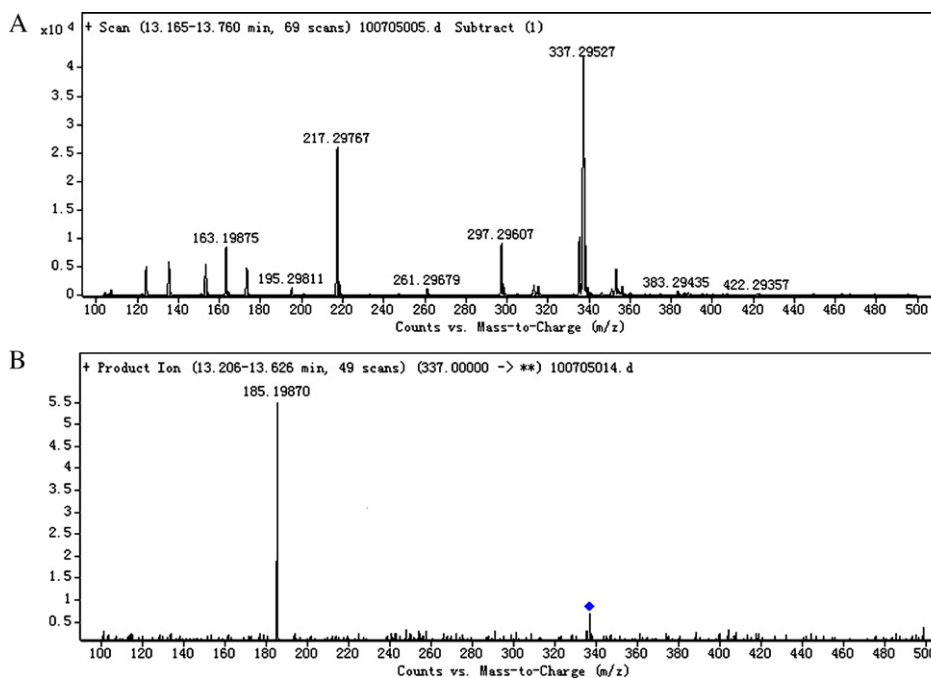


Fig. 6. (A) Mass spectrum and (B) MS/MS spectrum of Imp-III.

the epoxy compound, Imp-III formation was most probable due to auraptene epoxidation (Fig. 5B). In addition, formation of the product ions ( $m/z$  185) was deduced from Imp-III fragmentation (Fig. 7).

In positive ion full-scan mode, a protonated molecular ion peak was identified as  $(M+Na)^+$  peak at  $m/z$  355 in the mass spectrum of Imp-II (Fig. 8A). Molecular weight of Imp-II was 332, which was 18 amu more than Imp-III. In the MS/MS spectrum, an ion peak ( $m/z$  185) (Fig. 8B) derived from the charged parent ions ( $m/z$  355) was observed identical with the product ions of Imp-III and auraptene. As a result, Imp-II was suggested formed from Imp-III hydration,

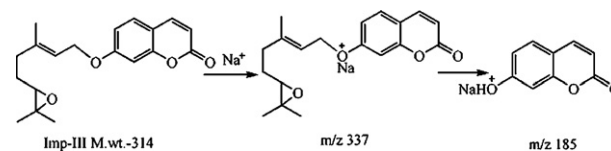


Fig. 7. Fragmentation mechanism for ions  $m/z$  185 formation from Imp-III.

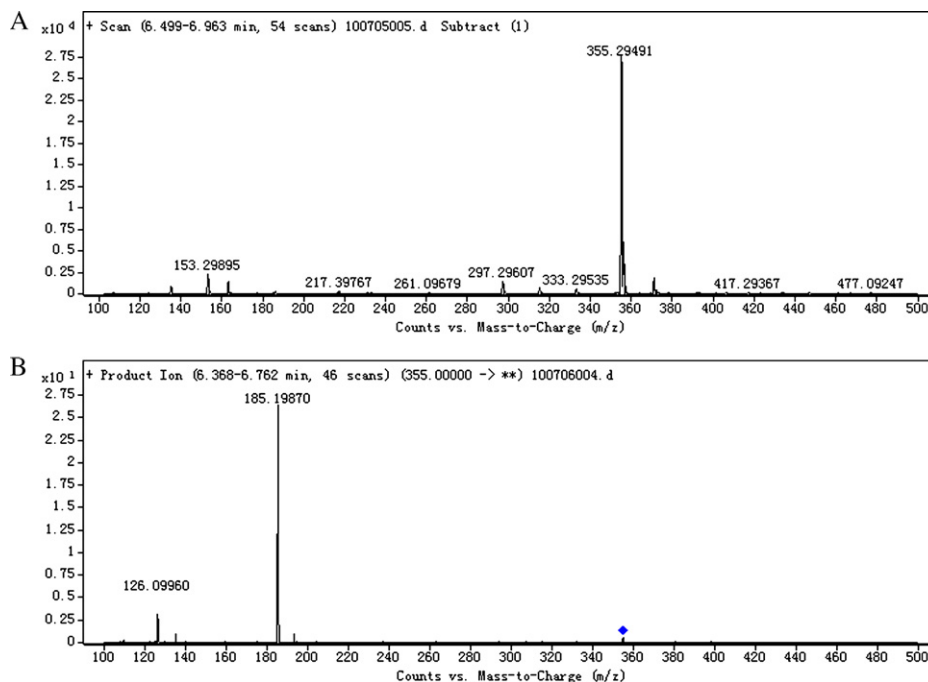


Fig. 8. (A) Mass spectrum and (B) MS/MS spectrum of Imp-II.



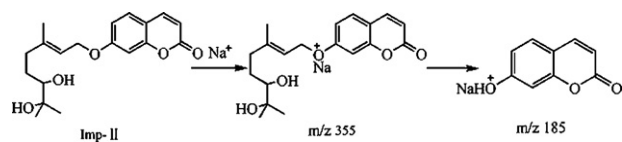


Fig. 9. Fragmentation mechanism for ions  $m/z$  185 formation from Imp-II.

i.e. Imp-III bearing an extra oxygen atom and two extra hydrogen atoms, or auraptene bearing two extra oxygen and two extra hydrogen. Since Imp-III can be easily hydrolyzed into a vicinal diol compound, Imp-II was supposed formed by Imp-III hydrolyzation (Fig. 5C), and the product ions ( $m/z$  185) may be yielded through Imp-II fragmentation (Fig. 9).

In positive ion full-scan mode, a protonated molecular ion peak was identified as  $(\text{M}+\text{H})^+$  peak at  $m/z$  313 in the mass spectrum of Imp-II (Fig. 10A). Molecular weight of Imp-IV was 312, which was 14 amu more than auraptene. In the MS/MS spectrum, a product ion peak at  $(\text{M}+\text{H})^+$   $m/z$  177 (Fig. 10B) was observed generated from the charged parent ion ( $m/z$  313); as a result, Imp-IV was suggested having only one extra  $-\text{CH}_3$  group than auraptene. Identity of this product ion peak  $(\text{M}+\text{H})^+$  at  $m/z$  177 was further confirmed by the HPLC chromatogram (see Supplementary Fig. 1).

The source of Imp-IV was found investigating the nature of the major impurity (Imp-V) in the synthesis of umbelliferone (Fig. 5D). Once detected, Imp-V was isolated by preparative HPLC and characterized by NMR (Table 1) and IR. In the IR spectrum, absorption bands were detected at 3158, 1680, 1600, 1516 and  $1451\text{ cm}^{-1}$  (data not shown).

The percent recoveries achieved from silica gel purification for Imp-III, Imp-II and Imp-IV were 95%, 57% and 55%, and chromatographic purities were proved to be 98%, 98.6% and 98.7%, respectively. Our observation showed that each synthesized chemical was identical to the one obtained from HPLC analysis in many ways, e.g. retention time, UV spectrogram, the mass and MS/MS spectrum. Moreover, the proposed structures of the three impurities were confirmed by IR,  $^1\text{H-NMR}$  and  $^{13}\text{C-NMR}$  spectral data (Tables 1 and 2) separately.

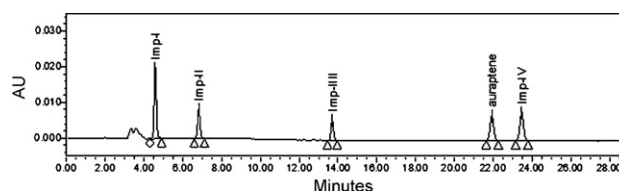


Fig. 11. Chromatogram for SST.

### 3.3. Validation of HPLC method

Validation of our developed analytic procedures according to the ICH guidelines [7] was carried out for Imp-I, II, III, IV and auraptene separately. Optimization of chromatographic separation was demonstrated by system suitability test (SST) (Fig. 11).

#### 3.3.1. Specificity

Forced degradation studies were conducted under a range of conditions, i.e. acid and base hydrolysis (dissolving in 1 mol/L HCl and 1 mol/L NaOH for 24 h at room temperature separately), heat ( $100^\circ\text{C}$  for 20 h), photolysis (4500 lx for 5 d) and oxidation (30%  $\text{H}_2\text{O}_2$ ).

In acid hydrolysis, 10 mL samples of auraptene API at concentration of  $200\ \mu\text{g}/\text{mL}$  were mixed with 1 mL HCl with 1 mol/L concentration, incubated at room temperature for 24 h, neutralized to pH 7.0 with 1 mol/L NaOH, and applied to chromatography analysis. Three completely separated feature peaks for impurities were detected at retention time 4.5 min, 5.4 min and 17.2 min (see Supplementary Fig. 2).

In base hydrolysis, 1 mL NaOH with 1 mol/L concentration were added to 10 mL samples of auraptene API at concentration of  $200\ \mu\text{g}/\text{mL}$ , and the mixture was incubated at room temperature for 24 h, neutralized to pH 7.0 with 1 mol/L HCl. The resulting solution was then analyzed by chromatography as described above. Three completely separated component peaks were identified for impurities at retention time 4.47 min, 6.06 min and 7.8 min (see Supplementary Fig. 2).

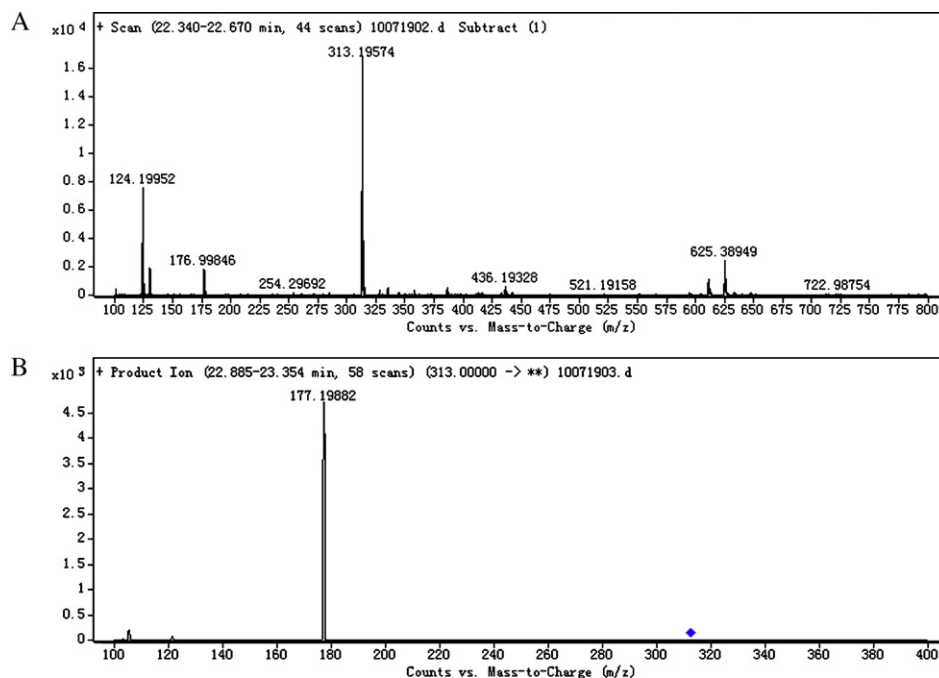


Fig. 10. (A) Mass spectrum and (B) MS/MS spectrum of Imp-IV.

**Table 1**  
NMR assignment of Imp-II, Imp-III, Imp-IV and Imp-V.

C <sup>a</sup>	Imp-II				Imp-III				Imp-IV				Imp-V			
	Number of protons (H)	$\delta_H$ (ppm)	$J^b$ (Hz)	$\delta_C$ (ppm)	Number of protons (H)	$\delta_H$ (ppm)	$J^b$ (Hz)	$\delta_C$ (ppm)	Number of protons (H)	$\delta_H$ (ppm)	$J^b$ (Hz)	$\delta_C$ (ppm)	Number of protons	$\delta_H$ (ppm)	$J^b$ (Hz)	$\delta_C$ (ppm)
2	–	–	–	161.3	–	–	–	161.2	–	–	–	161.3	–	–	–	161.2
3	1H	6.23	(dJ=9.6)	112.8	1H	6.23	(dJ=9.2)	112.9	1H	6.12	(dJ=8.8)	112.8	1H	6.04	(dJ=1.2)	113.3
4	1H	7.63	(dJ=9.2)	143.5	1H	7.63	(dJ=9.6)	143.4	–	–	–	142.2	–	–	–	155.4
5	1H	7.36	(dJ=8.4)	128.6	1H	7.35	(dJ=8.8)	128.6	1H	7.47	(dJ=8.8)	125.4	1H	7.52	(ddJ=2.4,8.8)	126.9
6	1H	6.83	(ddJ=2.4,8.4)	113.2	1H	6.83	(ddJ=2.4,8.4)	113.1	1H	6.87	(ddJ=2.8,8.4)	113.4	1H	6.75	(dJ=8.8)	113.7
7	–	–	–	161.9	–	–	–	161.9	–	–	–	161.8	–	–	–	163.3
8	1H	6.81	(dJ=2.8)	101.4	1H	6.81	(dJ=2.8)	101.4	1H	6.81	(dJ=2.8)	101.5	1H	6.63	(dJ=2.8)	102.9
9	–	–	–	155.7	–	–	–	155.7	–	–	–	155.1	–	–	–	155.9
10	–	–	–	112.3	–	–	–	112.4	–	–	–	111.7	–	–	–	110.7
11	–	–	–	–	–	–	–	–	3H	1.76	(s)	26.1	3H	2.36	(s)	18.1
1'	2H	4.59	(dJ=6.4)	63.3	2H	4.60	(dJ=6.4)	58.3	2H	4.59	(dJ=6.4)	65.3	–	–	–	–
2'	1H	5.51	(tJ=6.4)	142.1	1H	5.52	(tJ=8)	141.3	1H	5.47	(tJ=1.6)	152.5	–	–	–	–
3'	–	–	–	118.7	–	–	–	118.9	–	–	–	131.9	–	–	–	–
4'	2H	2.38	(m)	23.1	2H	2.24	(m)	18.6	2H	2.14	(m)	25.6	–	–	–	–
5'	2H	2.16	(m)	36.4	2H	1.68	(m)	36.1	2H	2.07	(m)	39.4	–	–	–	–
6'	1H	3.34	(dJ=10.4)	77.8	1H	2.72	(tJ=6)	65.2	1H	5.08	(tJ=1.2)	123.5	–	–	–	–
7'	–	–	–	73.1	–	–	–	63.8	–	–	–	118.3	–	–	–	–
8'	3H	1.21	(s)	29.3	3H	1.30	(s)	26.9	3H	1.68	(s)	18.6	–	–	–	–
9'	3H	1.17	(s)	26.4	3H	1.27	(s)	24.7	3H	1.60	(s)	17.6	–	–	–	–
10'	3H	1.78	(s)	16.7	3H	1.78	(s)	16.7	3H	2.39	(s)	16.7	–	–	–	–
	6'-OH	1.64	(m)	–	–	–	–	–	–	–	–	–	–	–	–	–
	7'-OH	1.48	(m)	–	–	–	–	–	–	–	–	–	–	–	–	–
	–	–	–	–	–	–	–	–	–	–	–	–	7-OH	12.9	(s)	–

<sup>a</sup> Refer the structural formula in Fig. 5 for numbering of carbon atoms.

<sup>b</sup> <sup>1</sup>H-<sup>1</sup>H coupling constant.

**Table 2**  
IR assignment and functional group.

Imp-II	Imp-III	Imp-IV	Functional group
3389	–	–	–OH
1706	1708	1730	
1614, 1507, 1462	1612, 1509, 1457	1618, 1508, 1443	
–	1278, 843	–	

**Table 3**  
The contents (%) of the four impurities in auraptene ( $n = 3$ ).

No.	Sample number	Imp-I	Imp-II	Imp-III	Imp-IV
1	20090331	0.010827	0.011789	0.012052	0.015817
2	20090401	0.011535	0.012492	0.013958	0.016986
3	20090409	0.012035	0.013248	0.01389	0.016542
4	20090413	0.012286	0.013427	0.01496	0.019704
5	20090416	0.011764	0.012985	0.013288	0.016318

In heat treatment, 10 mL samples of auraptene API at concentration of 200  $\mu\text{g/mL}$  were kept under reflux for 20 h at 100  $^{\circ}\text{C}$ , and then analyzed by chromatography. A feature peak for impurity was recognized at retention time 23.4 min (Supplementary Fig. 2).

In oxidation test, 10 mL samples of auraptene API at concentration of 200  $\mu\text{g/mL}$  were diluted in 2 ml 30%  $\text{H}_2\text{O}_2$ . Then the solution was neutralized to pH 7.0, and then analyzed by chromatography. Individual peaks were recognized at retention time 4.54 min, 6.67 min, 11.50 min, 11.99 min and 17.82 min (see Supplementary Fig. 2).

In photolytic stability test, 10 mL samples of auraptene API at concentration of 200  $\mu\text{g/mL}$  were stored under illumination of  $4500 \pm 500$  lx for five days. When the solution was analyzed by chromatography, several impurity peaks were achieved (see Supplementary Fig. 2).

In above forced degradation studies, our examination showed that all degraded products were well separated from each other, all impurity lines could gain effective baseline separation from the chief constituent peak under the tested conditions (see Supplementary Fig. 2). This has indicated the stability and specificity of the established chromatography conditions.

### 3.3.2. Precision and accuracy

In system precision measurement, 10  $\mu\text{L}$  standard solution was injected in six replicates on the same chromatography condition to check the Relative Standard Deviation (RSD). The RSD for these impurities, i.e. 0.25% for Imp-I, 0.64% for Imp-II, 0.50% for Imp-III and 1.74% for Imp-IV, were all within the generally acceptable limit of 5%.

System accuracy was assessed for the related substances by spiking of known amounts of an impurity in samples of auraptene API (test preparation) at levels, 80%, 100% and 120% of the specified limit. The recoveries of impurities were calculated from the equation, i.e.  $R_{(i)}\% = \frac{[C_{\text{obs}(i)} \text{ in spiked sample} - C_{\text{obs}(i)} \text{ in unspiked sample}]}{C_{\text{spike}(i)}} \times 100$ , where  $R_{(i)}$  was the recovery for sample  $i$ ,  $C_{\text{obs}(i)}$  was the concentration of the analyte observed for sample  $i$ , and  $C_{\text{spike}(i)}$  was the concentration of the spike added to sample  $i$ . Mean recoveries for Imp-I, Imp-II, Imp-III and Imp-IV at 80% level were calculated as 102.2%, 100.1%, 101.4% and 99.2%, at 100% level were 105.7%, 101.0%, 101.2% and 100.9%, and at 120% level were 101.9%, 101.2%, 100.1% and 99.8%, respectively. The results showed the assay was satisfactory with the mean recovery from 99.2% to 105.7% with R.S.D. less than 1.63% for the mean recovery.

### 3.3.3. Linearity, LOD and LOQ

The linear regression and linearity plot was estimated for each impurity ( $r > 0.9995$ ). The regression equations were calculated in the form of  $Y = aX + b$ , where  $X$  and  $Y$  are the injecting amount of the standard solution and the corresponding peak area, and  $a$  and  $b$  are the slope and the intercept, respectively. Good calibration curves of impurity standard solutions were obtained. The regression equations for Imp-I, Imp-II, Imp-III and Imp-IV were  $Y = 100.48X + 7.8609$  ( $R^2 = 0.9998$ ),  $Y = 54.098X + 0.2236$  ( $R^2 = 9997$ ),  $Y = 57.199X + 6.1133$  ( $R^2 = 9998$ ) and  $Y = 57.149X + 11.15$  ( $R^2 = 9991$ ), respectively. The calibration curves proved to be linear in the range of 2.07–20.72  $\mu\text{g/mL}$  for Imp-I, 2.08–20.8  $\mu\text{g/mL}$  for Imp-II, 1.98–19.8  $\mu\text{g/mL}$  for Imp-III and 2.156–21.56  $\mu\text{g/mL}$  for Imp-IV.

The limit of detection (LOD) and the limit of quantification (LOQ) were by a series of diluted mixed standards. The signal-to-noise ratios were presented as 3:1 for LOD and 10:1 for LOQ (measured by concentration). The LOQ values were 1.01 ng for Imp-I, 3.33 ng for Imp-II, 2.77 ng for Imp-III and 4.31 ng for Imp-IV. The LOD values were 0.43 ng for Imp-I, 0.87 ng for Imp-II, 0.82 ng for Imp-III and 1.13 ng for Imp-IV.

### 3.3.4. Quantification of impurities

The established method has been applied to quantification of the four impurities in auraptene. When we calculated from the corresponding calibration curve, content of each analyte was proved within the impurity limit in the ICH guidelines (Table 3). This result indicated that the auraptene purification process in our laboratory was feasible and stable; moreover, quality of our synthesized auraptene was consistent with the standards for pharmaceutical ingredients.

## 4. Conclusion

Impurities in bulk drug must be limited or controlled for quality and safety considerations. In this paper, impurities in auraptene were isolated, identified, synthesized and quantified by spectroscopic techniques. SST was conducted for auraptene quality control, and optimized conditions were employed in spectroscopic assays. A stability-indicating analytical procedure was developed after forced degradation studies, and then was validated according to the ICH guidelines. This established procedure could be conveniently used for the quantitative determination of process-related substances in auraptene.



## Acknowledgement

The authors gratefully acknowledge financial support from National Natural Science Foundation of China (no. 30660230).

## Appendix A. Supplementary data

Supplementary data associated with this article can be found, in the online version, at doi:10.1016/j.jpba.2011.05.011.

## References

- [1] K. Nagao, N. Yamano, B. Shirouchi, N. Inoue, S. Murakami, T. Sasaki, T. Yanagita, J. Agric. Food. Chem. 58 (2010) 9028–9032.
- [2] F. Epifano, S. Genovese, M. Curini, Auraptene: phytochemical and pharmacological properties, in: T. Matsumoto (Ed.), *Phytochemistry Research Progress*, Nova Biomedical Books, 2008, pp. 145–162.
- [3] P. Krishnan, K.J. Yan, D. Windler, J. Tubbs, R. Grand, B.D. Li, C.M. Aldaz, J. McLarty, H.E. Kleiner-Hancock, BMC Cancer 29 (2009), p. 259.
- [4] K. Hayashi, R. Suzuki, S. Miyamoto, Y. Shin-Ichiroh, H. Kohno, S. Sugie, S. Takashima, T. Tanaka, Nutr. Cancer 58 (2007) 75–84.
- [5] M. Curin, G. Carvotto, F. Epifano, G. Giannone, Curr. Med. Chem. 13 (2006) 199–222.
- [6] P. Zhang, Y. Li, M. Tu, Y. Zhang, H. Chen, W. Yang, Lishizhen Med. Mater. Med. Res. 21 (2010) 1851–1853.
- [7] ICH Harmonised Tripartite Guideline, Impurities in New Drug Substances, Q3A (R2), Current Step 4 version, 25 October 2006.
- [8] K. Pilaniya, H.K. Chandrawanshi, U. Pilaniya, P. Manchandani, P. Jain, N. Singh, J. Adv. Pharm. Technol. Res. 1 (2010) 302–310.
- [9] Y. Li, P. Zhang, H. Chen, F. Wang, L. Wei, M. Tu, W. Yang, J. Jiangxi Univ. TCM 21 (2009) 43–45.